FULL-BRIDGE THREE-PORT CONVERTERS WITH WIDE INPUT VOLTAGE RANGE FOR RENEWABLE POWER SYSTEMS

Dr. A.N. Malleswara Rao

Professor in EEE, SKEC, Khammam(India)

ABSTRACT

A systematic method for deriving three-port converters (TPCs) from the full-bridge converter (FBC) is proposed in this project. The proposed method splits the two switching legs of the FBC into two switching cells with different sources and allows a dc bias current in the transformer. By using this systematic method, a novel full-bridge TPC (FB-TPC) is developed for renewable power system applications, which features simple topologies and control, a reduced number of devices, and single-stage power conversion between any two of the three ports. The proposed FB-TPC consists of two bidirectional ports and an isolated output port. The FB-TPC is analyzed in detail with operational principles, design considerations, and a pulse width modulation scheme (PWM), which aims to decrease the dc bias of the transformer. Experimental results verify the feasibility and effectiveness of the developed FB-TPC. The topology generation concept is further extended, and some novel TPCs, dual-input, and multiport converters are presented.

I. INTRODUCTION

Renewable power systems, which are capable of harvesting energy from, for example, solar cells, fuel cells, wind, and thermoelectric generators, are found in many applications such as hybrid electric vehicles, satellites, traffic lights, and powering remote communication systems [1]. Since the output power of renewable sources is stochastic and the sources lack energy storage capabilities, energy storage systems such as a battery or a super capacitor are required to improve the system dynamics and steady-state characteristics [2]. A three-port converter (TPC), which can interface with renewable sources, storage elements, and loads, simultaneously, is a good candidate for a renewable power system and has recently attracted increased research interest [3]. Compared with the conventional solutions that employ multiple converters, the TPC features single-stage conversion between any two of the three ports, higher system efficiency, fewer components, faster response, compact packaging, and unified power management among the ports with centralized control. As a result of these remarkable merits, many TPCs have been proposed recently for a variety of applications [4]. One way to construct a TPC is to interface several conversion stages to a common dc bus. But this is not an integrated solution since only a few devices are shared [5]. Some TPCs are constructed from full-bridge, half-bridge, or series-resonant topologies by utilizing the magnetic coupling through a multi winding transformer. Power flow control and zero-voltage switching (ZVS) are achieved with phase-shift control between different switching bridges, whose principles are the same as the dual active-bridge (DAB) topology. Isolation and bidirectional capabilities can also be achieved with these topologies [6]. However, too many active switches have been used,

resulting in a complicated driving and control circuit, which may degrade the reliability and performance of the integrated converters. In a boost-integrated TPC is proposed based on the phase-shift full-bridge converter (FBC) and power flow control is implemented with pulse width modulation (PWM) plus phase-shift control. This principle is further extended to the three-phase FBC [7]. A tri-modal half-bridge converter is developed from a half-bridge converter to implement three-port interface. This converter can be regarded as a buck integrated TPC because the primary circuit of the half-bridge converter functions as a buck converter to bridge the power flow path between the input source and the battery. These TPCs offer low component counts and simple control [8],[9]. However, because the equivalent conversion circuit between the input source and energy storage element is a step-up or step-down converter with limited voltage conversion ratio, they are not flexible enough for applications where the voltage of the source port, such as solar, fuel cells, and thermoelectric generator, varies over a wide range [10].

II. PROPOSED TOPOLOGY

The major contribution of this project is to propose a systematic method for generating TPC topologies from FBCs and to find a novel full bridge TPC (FB-TPC) with single-stage power conversion between any

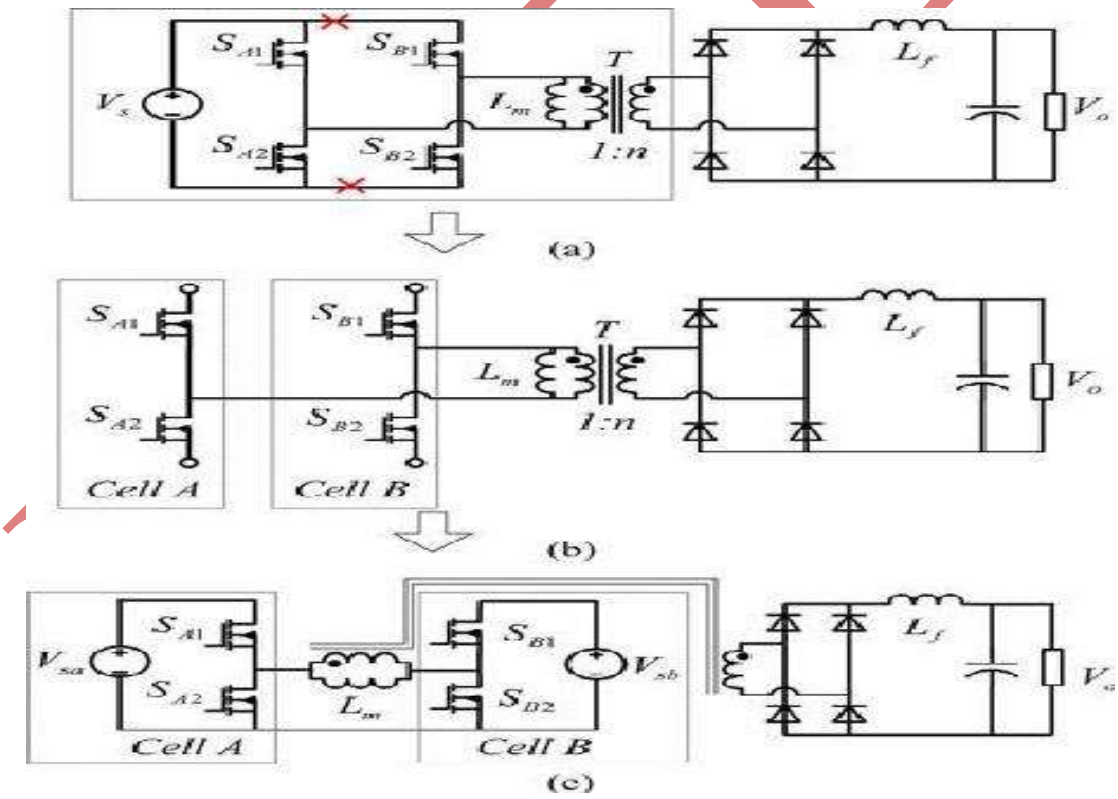

Fig.1 Proposed Derivation Of Full-Bridge Three-Port Converter (A) Full-Bridge Converter (B) Two-Switching Cells (C) Full-Bridge Three-Port Converter

two of the three ports. Furthermore, from a topological point of view, because a buck-boost converter is integrated in the proposed FB-TPC, it can adapt to applications with a wide source voltage range [11]. ZVS of all the primary-side switches can also be achieved with the proposed FB-TPC. This project is organized as follows.

III. FB-TPC FROM A FULL-BRIDGE DC-DC CONVERTER

Referring to Fig.1(a), the primary side of the FBC consists of two switching legs, composed of S_{A1} , S_{A2} and S_{B1} , S_{B2} , in parallel, connected to a common input source V_s. For the primary side of the FBC, the constraint condition of the operation of the FBC is the voltage-second balance principle of the magnetizing inductor L_m. This means that, from a topological point of view, the two switching legs of the FBC can also be split into two symmetrical parts, cells A and B, if only L_m satisfies the voltage-second balance principle, as shown in Fig.1(b). The two cells can be connected to different sources, V_{sa} and V_{sb} , respectively, as shown in Fig.1(c), and then a novel FB-TPC is derived [12]. The voltage of the two sources of the FB-TPC can be arbitrary. Specially, if V_{sa} always equals V_{sb} , the two cells can be paralleled directly and then the conventional FBC is derived. Therefore, the FBC can be seen as a special case of the FB-TPC as shown in Fig.1(c).

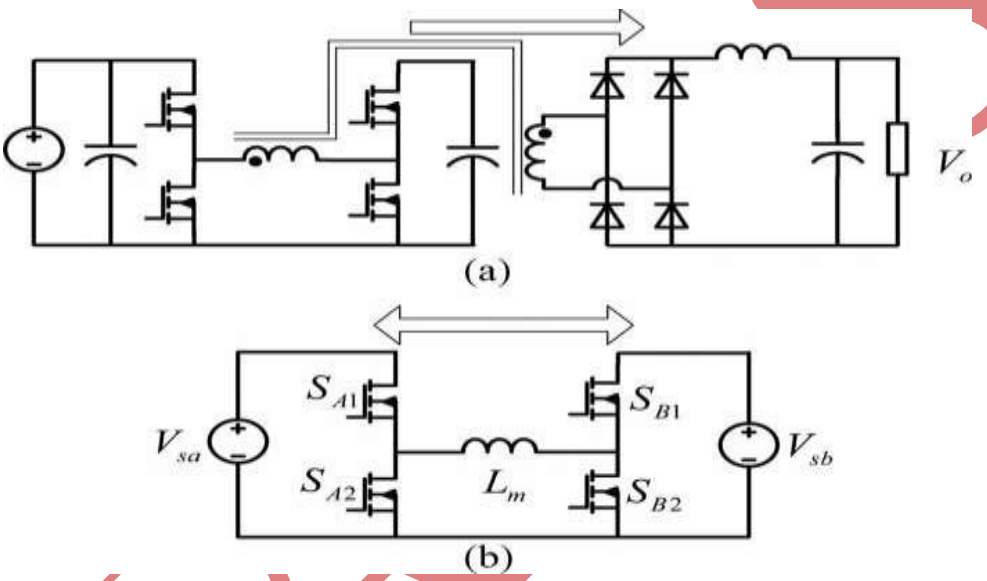

Fig.2 Equivalent Circuits (A) Between Source And Load. (B) Between The Two Sources

Close observation indicates that the FB-TPC has a symmetrical structure and both V_{sa} and V_{sb} can supply power to the load V_o. The equivalent circuit from one of the source ports to the load port is shown in Fig.2(a). In addition, a bidirectional buck-boost converter is also integrated in the primary side of the FB-TPC by employing the magnetizing inductor of the transformer L_m as a filter inductor. With the bidirectional buck-boost converter, the power flow paths between the two sources, V_{sa} and V_{sb} , can be configured and the power can be transferred between V_{sa} and V_{sb} freely [13]. The equivalent circuit between the two sources is illustrated in Fig.2(b). According to the equivalent circuits shown in Fig.2, it can be seen that the power flow paths between any two of the three ports, V_{sa}, V_{sb}, and V_o have been built. The unique characteristics of the FB-TPC are analyzed and summarized as follows.

1) The FB-TPC has two bidirectional ports and one isolated output port. Single-stage power conversion between any two of the three ports is achieved. The FB-TPC is suitable for renewable power systems and can be connected with an input source and an energy storage element, such as the photovoltaic (PV) with a battery backup, or with two energy storage elements, such as the hybrid battery and the super capacitor power system.

2) A buck-boost converter is integrated in the primary side of the FB-TPC. With the integrated converter, the

source voltage V_{sa} can be either higher or lower than V_{sb}, and vice versa. This indicates that the converter allows the sources' voltage varies over a wide range.

3) The devices of the FB-TPC are the same as the FBC and no additional devices are introduced which means high integration is achieved.

4) The following analysis will indicate that all four active switches in the primary side of the FB-TPC can be operated with ZVS by utilizing the energy stored in the leakage inductor of the transformer, whose principle is similar to the phase-shift FBC.

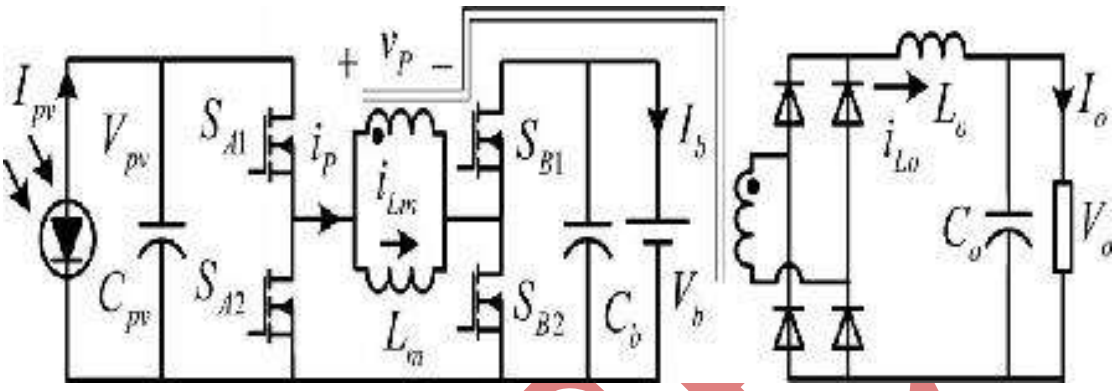

Fig.3 Topology Of The Proposed FB-TPC

IV. ANALYSIS OF THE FB-TPC FOR THE STAND-ALONE RENEWABLE POWER SYSTEM APPLICATION

The FB-TPC, as shown in Fig.2 (b), is applied to a stand-alone PV power system with battery backup to verify the proposed topology. To better analyze the operation principle, the proposed FB-TPC topology is redrawn in Fig.3, the two source ports are connected to a PV source and a battery, respectively, while the output port is connected to a load [14]. There are three power flows in the standalone PV power system: 1) from PV to load; 2) from PV to battery; and 3) from battery to load. As for the FB-TPC, the load port usually has to be tightly regulated to meet the load requirements, while the input port from the PV source should implement the maximum power tracking to harvest the most energy [14]. Therefore, the mismatch in power between the PV source and load has to be charged into or discharged from the battery port, which means that in the FB-TPC, two of the three ports should be controlled independently and the third one used for power balance. As a result, two independently controlled variables are necessary.

4.1. Switching State Analysis

Ignoring the power loss in the conversion, we have

$$P_{pv} = P_b + P_o \quad (1)$$

where P_{pv} , P_b , and P_o are the power flows through the PV, battery, and load port, respectively. The FB-TPC has three possible operation modes: 1) dual-output (DO) mode, with $p_{pv} \geq p_o$, the battery absorbs the surplus solar power and both the load and battery take the power from PV; (2) dual-input (DI) mode, with $p_{pv} \leq p_o$ and

$p_{pv} > 0$, the battery discharges to feed the load along with the PV; and (3) single-input single-output (SISO) mode, with $p_{pv} = 0$, the battery supplies the load power alone. When $p_{pv} = p_o$ exactly, the solar supplies the load power alone and the converter operates in a boundary state of DI and DO modes. This state can either be treated as DI or DO mode. Since the FB-TPC has a symmetrical structure, the operation of the converter in this state is the same as that of SISO mode, where the battery feeds the load alone. The operation modes and power flows of the converter are listed in Table I. The power flow paths/directions of each operation mode have been illustrated in Fig.4. The switching states in different operation modes are the same and the difference between these modes are the value and direction of i_{Lm}, as shown in Fig. 3, which is dependent on the power of p_{pv} and p_o . In the DO mode, i_{Lm} is positive, in the SISO mode, i_{Lm} is negative, and in the DI mode, iL_m can either be positive or negative. Take the DO mode as an example to analyze.

Table I: Operation Modes Of The Fb-Tpc

Operation modes	Power of PV	Power of battery
Dual-output mode	$P_{pv} \geq P_o$	Battery charging, $P_b \geq 0$
Dual-input mode	$P_{pv} \leq P_o$, $P_{pv} > 0$	Battery discharging, $P_b < 0$
Single-input Single-output mode	$P_{pv} = 0$	Battery discharging, $P_b = -P_o$

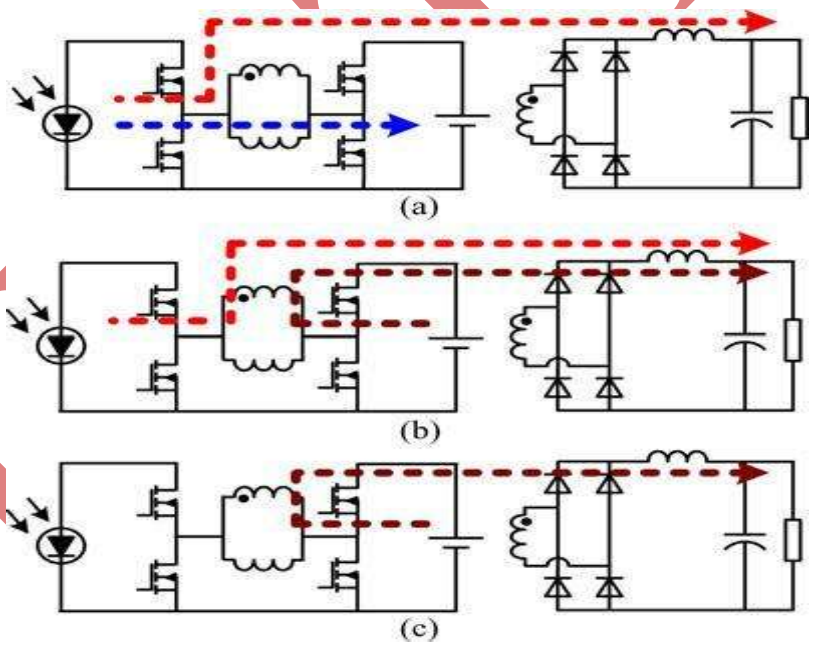

Fig.4. Power Flow Paths/Directions Of Each Operation Mode (A) DO Mode (B) DI Mode (C) SISO Mode

For simplicity, the following assumptions are made: 1) C_{pv} , C_b , and C_o are large enough and the voltages of the three ports, V_{pv} , V_b , and V_o , are constant during the steady state; and 2) the $V_{pv} \geq V_b$ case is taken as an example for the switching state analysis.

4.2. ZVS Analysis

According to the analysis, the operation of the FB-TPC is similar to the operation of a phase-shift FBC with the

two switches S_{A1} (S_{B1}) and S_{A2} (S_{B2}), driven with complementary signals. The proposed FB-TPC can utilize the leakage inductance, filter inductance, and the output capacitors (parasitic drain to source capacitors) of the switches to realize ZVS, zero-voltage turn-ON, and zero-voltage turn-OFF for all the switches. The operation principle is similar to the phase-shift FBC. The only difference is that in the proposed FB-TPC, the magnetizing inductor of the transformer L_m can also help to achieve ZVS of the switches if the direction of i_{Lm} is the same as i_P.

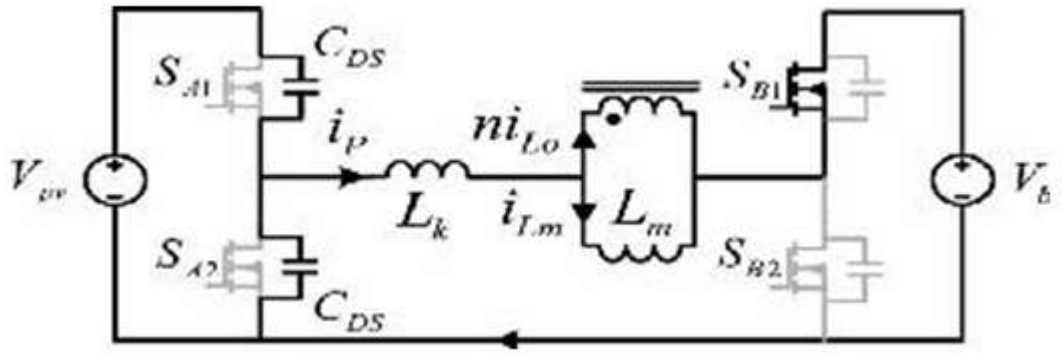

Fig.5. ZVS Analysis Of *SA* 2

Take S_{A2} as an example. As shown in Fig.6, where only the primary circuit is shown for simplicity, considering the leakage inductance L_k , when S_{B1} is ON and S_{A1} is turned OFF, $i_P = i_{Lm} + ni_{Lo}$, the energy stored in L_k and L_m will release to charge or discharge the parasitic drain to source capacitors of S_{A1} and S_{A2} . As a result, with a proper dead

time, ZVS of S_{A2} can be achieved if the following condition is satisfied.

$$\frac{1}{2}\left[L_k\left(i_{Lm}+ni_{Lo}\right)^2+L_m i_{Lm}^2\right] > C_{DS}V_b^2 \qquad (2)$$

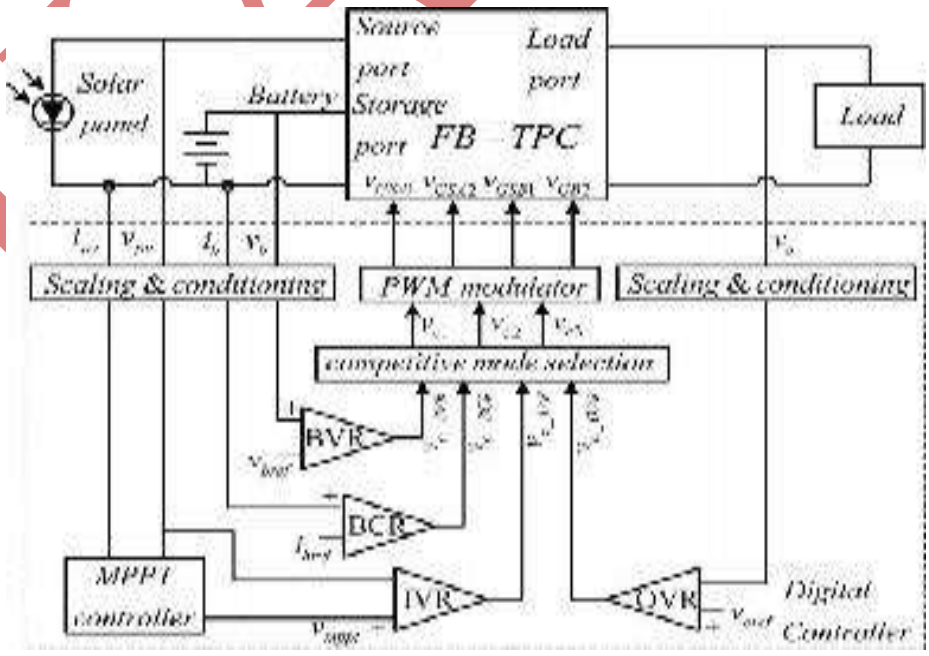

Fig.6. Control Diagram For The Three-Port Converter

4.3. Pulse width Modulation

The power management and the control for the TPC proposed in are applied to the FB-TPC because the power control of the renewable power system with battery backup follows a similar principle and has nothing to do with the type of topology. However, the PWM schemes of different converters are usually different from each other and mainly determined by the topology. For better analysis of the PWM scheme of the FB-TPC, the control diagram for the power system is redrawn in Fig.6. Four regulators, PV voltage regulator (IVR) for MPPT, battery voltage regulator (BVR) for maximum voltage charging control, battery current regulator (BCR) for maximum current charging control, and output voltage regulator (OVR) for output voltage control, are used to implement the power management of the system. With the control diagram shown in Fig.7, the FB-TPC can work in the DO, DI, or SISO mode, depending on the relationship between the PV power and load power [15]. Different PWM schemes can be applied to the proposed FBTPC. However, i_{Lm} can be decreased by increasing D_{A1} and D_{B1}. To decrease the magnetizing inductor's current of the transformer, D_{A1} and D_{B1} should be as large as possible. According to the switching state analysis, it can be seen that, as shown in Fig.7, the smaller the D_1, the larger the D_{B1}; therefore, the maximum value of D_{B1} is

$$D_{B1\_max} = D_{A1} + D_3 \tag{3}$$

and the maximum value of D_{A1} is determined by D_3

$$D_{A1\_max} = 1 - D_3 \tag{4}$$

Based on the analysis, the proposed PWM scheme and its generation are illustrated in Fig.7, where V_{tri} is the peak-to-peak value of the carrier voltage V_{tri} , and V_{c1} , V_{c2} , V_{c3} are control voltages generated by using a competitive method and given by the following equations:

$$\begin{aligned} V_{C1} &= \max(V_{C\_BVR}, V_{C\_BCR}, V_{C\_IVR}) \\ V_{C2} &= \min(V_{C2}, V_{tri}) \\ V_{C3} &= \max(0, V_{C2} - V_{tri}) \end{aligned} \tag{5}$$

With the proposed PWM scheme, when V_{pv} is much higher than V_b , $V_{c2} < V_{tri}$, and V_{c3} stays at zero, D_{B1} will reach its maximum value, given by (3), as shown in Fig. 7(b). There are only three switching states, states II–IV, in one switching cycle. This means that by regulating the turned OFF time of S_{A1} with V_{c1} , the PV power can be controlled to achieve the MPPT, or battery charging control and output voltage V_o is further controlled with V_{c2}regulating D_3 by adjusting the turned OFF time of S_{B1} .When V_{pv} decreases and $V_{c2} \leq V_{tri}$, D_{A1} will reach its maximum value, given by (4), $V_{c2} = V_{tri}$ and $V_{c3} \geq 0$, then V_o is controlled with V_{c2} by regulating the turned ON time of S_{B1} , as shown in Fig.7(b), and there are three switching states, states I–III, in one switching cycle. With the proposed PWM scheme, the converter can adapt to different input voltages while minimizing the magnetizing inductor's current of the transformer.

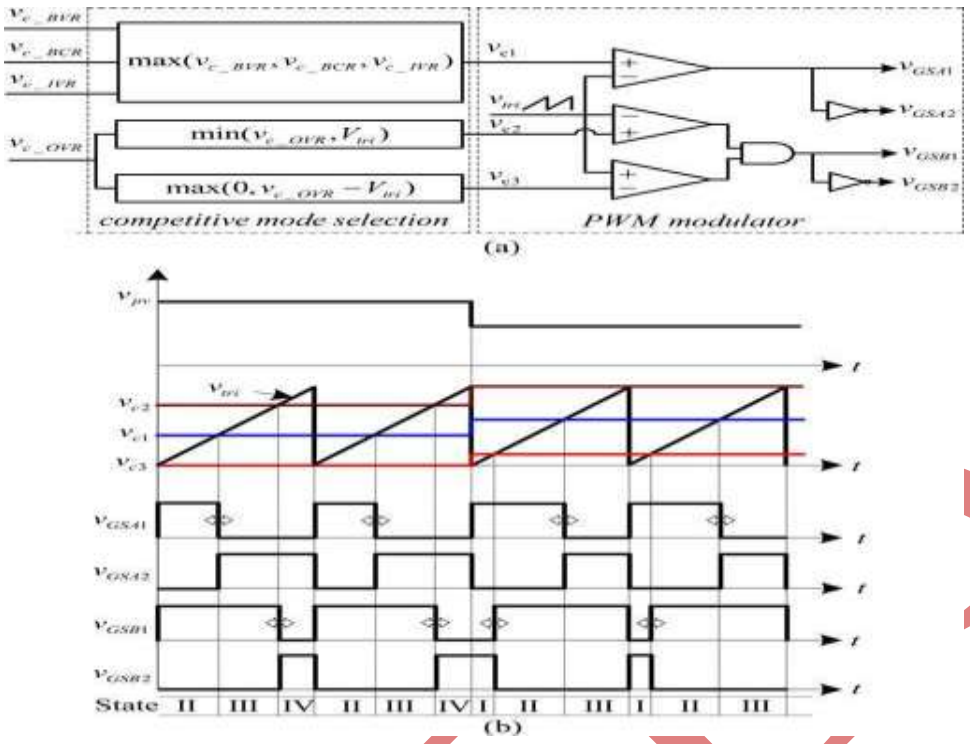

Fig.7 PWM Scheme For The FB-TPC (A) PWM Generation (B) Key Waveforms

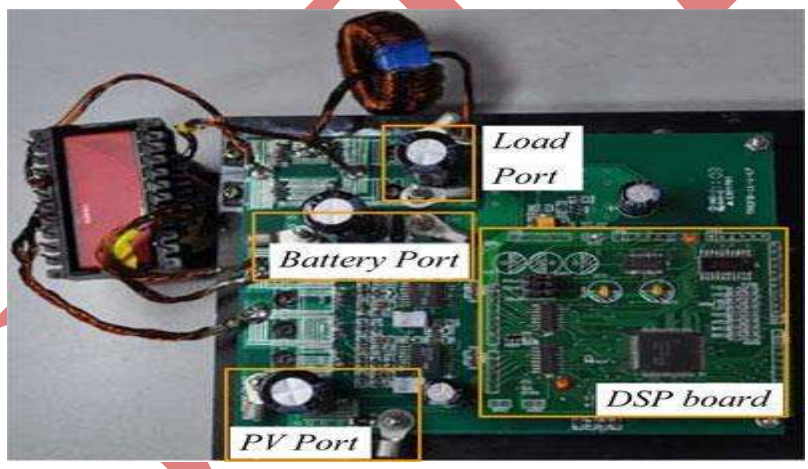

Fig.8. Picture Of The Prototype

TABLE II: CIRCUIT PARAMETERS

V_{pv}	38 V~76 V	P_{in}	0~300 W
V_o	42 V	P_o	0~180W
V_b	26 V~38 V	C_{pv}, C_b, C_o	470µF
L_m	70µH	L_o	100µH
Turns ratio (n)	3:4	S_{A1}, S_{A2}, S_{B1}, S_{B2}	IRF3710
Rectifier diodes	SRF20200C	Switching frequency	100 KHZ

V. EXPERIMENTAL RESULTS

An FB-TPC prototype controlled by a TMS320F2808 DSP, as shown in Fig.8, is built with the key parameters listed in Table II. A variable resistor in series with a dc source is used to simulate the PV characteristics. The steady-state waveforms of the converter with 55V input voltage at full load are shown in Fig. 9.

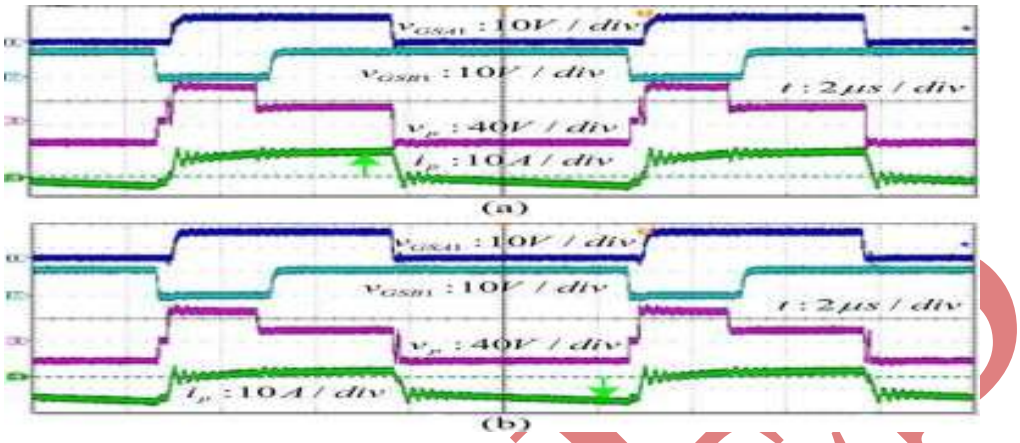

Fig.9 Steady-State Waveforms At 55V Input Voltage With Full-Load Condition In (A) Dual-Output Mode And (B) Dual-Input Mode.

Fig.9(a) shows the waveforms under the DO mode and Fig. 9(b) shows the waveforms of the DI mode. It can be seen that the shapes of the corresponding waveforms are the same and the only difference is the average value of the primary winding's current ip . In Fig.9(a), the average value of i_p is positive while in Fig. 9(b) i_p is negative. With this input voltage, $V_{c2} \leq V_{tri}$ and D_{A1} reaches its maximum value, the converter switches among states I–III alternately in one switching cycle, as shown in the right part of Fig. 9(b).

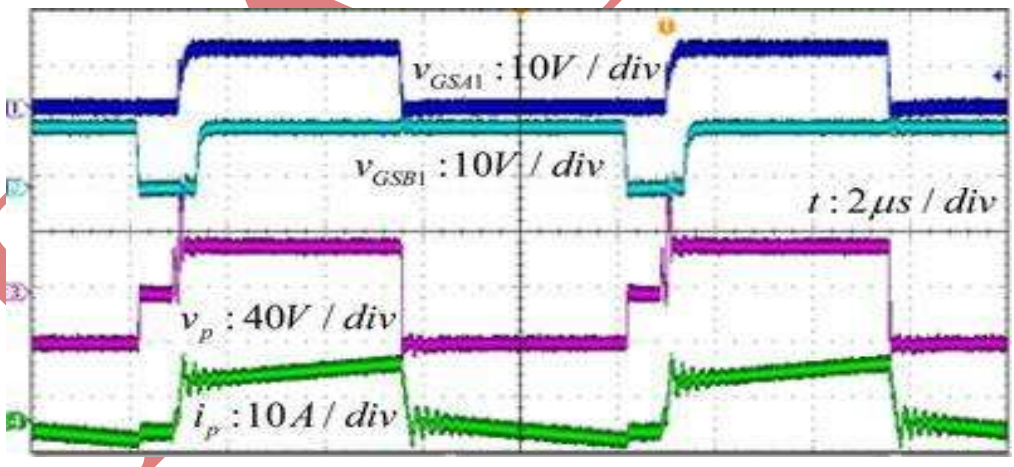

Fig.10. Steady-State Waveforms At 70V Input Voltage With Full-Load Condition In Dual-Output Mode

The steady-state waveforms of the converter in DO mode with 70V input voltage at full load are given in Fig.10. With this input voltage, $V_{c2} > V_{tri}$ and D_{B1} reaches its maximum value. The converter switches among states II–IV alternately in one switching cycle, as shown in the left part of Fig. 9(b).

The driving voltage and drain to source voltage on S_{A1}, S_{A2} , S_{B1} , and S_{B2} , in the DO mode at full load, is given in Fig.11, which indicates that all the switches are turned ON with ZVS and the voltage spike on switches is very small when switches are turned OFF.

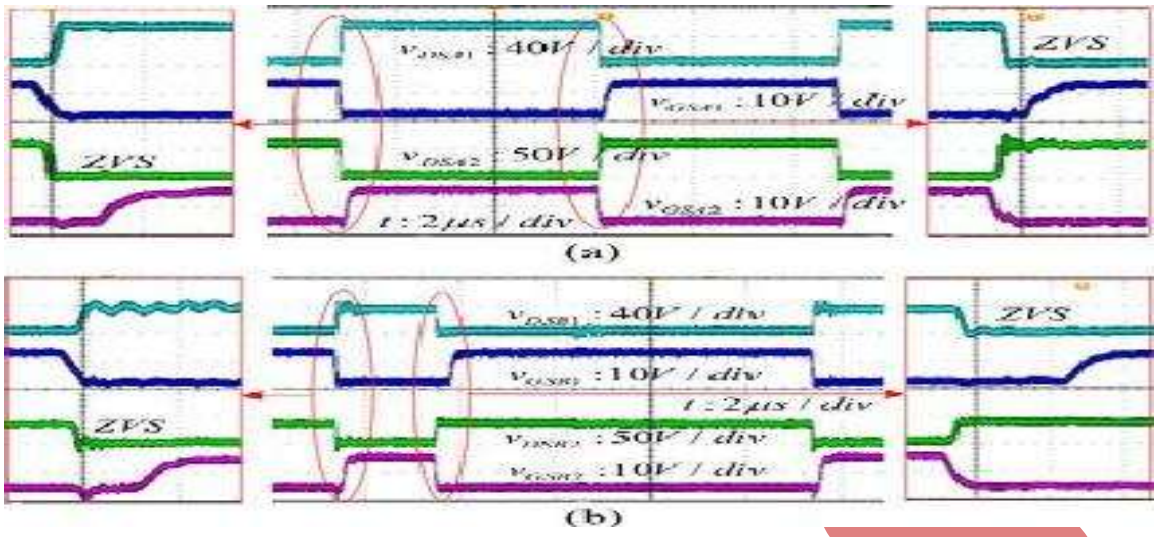

Fig11 Driving Voltage And Drain To Source Voltage Of (A) *SA* 1 And *SA* 2 And (B) *SB* 1 And *SB* 2.

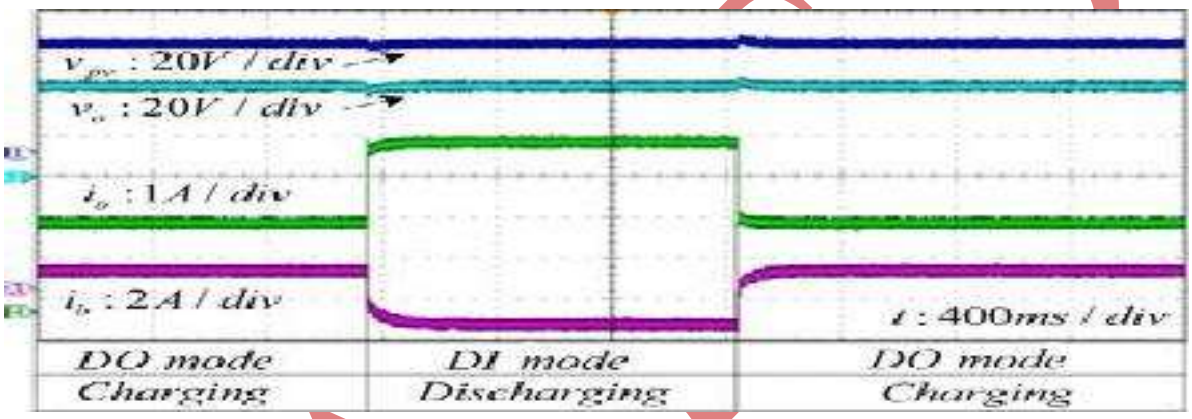

Fig.12 Load Transient Waveforms By Stepping Up (Half Load To Full Load) And Stepping Down (Full Load To Half Load) Load Resistors.

Fig.12 shows the transient waveforms with stepping up (from half load to full load) and stepping down (from full load to half load) the load resistors. It can be seen that when the output load transitions between half load and full load, the converter switches between DI mode and DO mode, and the battery transients between charging mode and discharging mode. The input power is kept constant, and the output voltage is stable during the load transient as while the battery current/power varies to compensate for the load power.

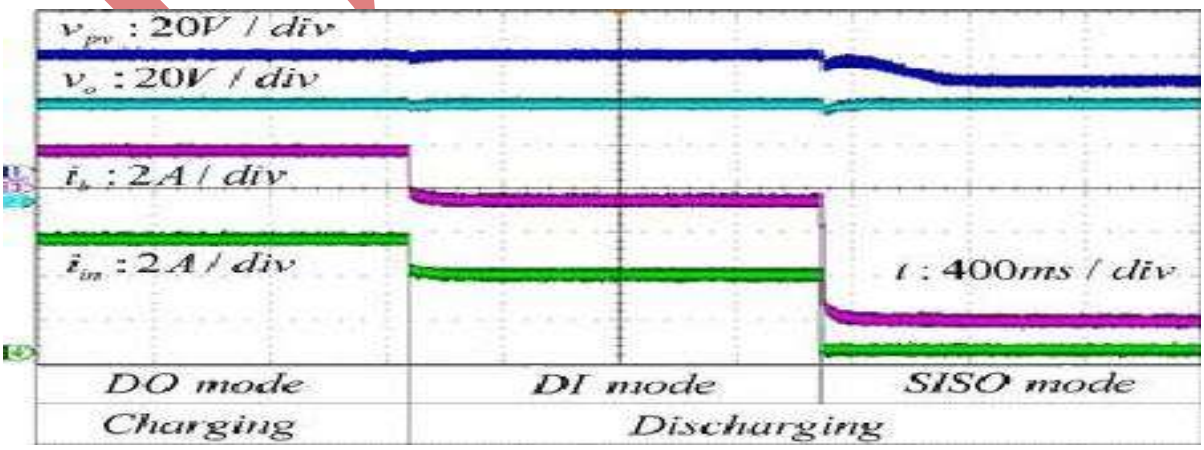

Fig.13. Waveforms Of Operation Mode Transition: Dual-Output Mode To Dual Input Mode And Then To SISO Mode.

The operation mode switching among the DO, DI, and SISO are also tested, and the waveforms are given in Fig.13. It can be seen that the output voltage *vo* is always tightly controlled under every operation mode and also during mode transients.

VI. CONCLUSION

Novel FB-TPCs have been proposed and investigated in this project. The FB-TPCs are rooted in the FBC and generated by splitting the two switching legs of the FBC into two switching cells, connecting the two cells to different sources, and utilizing the magnetizing inductance of the transformer as a filter inductor. A Full-bridge converter implemented with Three-port Full-bridges has been proposed in this project. A control method has been presented for achieving soft switching over a wide input range. A PWM control method is applied to the Three-port Full-bridge converter. The particular structure of a boost Full-bridge, interfaces the port having a wide operating voltage, makes it possible to handle voltage variations at this port by adjusting the duty cycle of all the three Full-bridges. With this approach, the operation of the converter is optimized with both current stress and rms loss being reduced. Moreover, soft-switching conditions for all switches are achievable over the entire phase shift region. Control scheme based on multiple PI regulators manages the power flow, regulates the output, and adjusts the duty cycle in response to the varying voltage on the port. Simulation and experimental results were presented, validating the effectiveness of the proposed converter and its control scheme.

REFERENCES

[1] Kwasinski, "Quantitative evaluation of DC micro grids availability: Effects of system architecture and converter topology design choices," *IEEE Trans. Power Electron.*, vol. 26, no. 3, pp. 835–851, Mar. 2011.

[1] W. Jiang and B. Fahimi, "Multi-port power electric interface for renewable energy sources," in *Proc. IEEE Appl. Power Electron. Conf.*, 2009, pp. 347–352.

[2] W. Jiang and B. Fahimi, "Multiport power electronic interface Concept, modeling and design," *IEEE Trans. Power Electron.*, vol. 26, no. 7, pp. 1890–1900, Jul. 2011.

[3] H. Tao, J. L. Duarte, and M. A. M. Hendrix, "Multiport converters for hybrid power sources," *IEEE Proc. Power Electron. Spec. Conf.*, pp. 3412– 3418, 2008.

[4] H. Tao, A. Kotsopulos, J. L. Duarte, and M. A. M. Hendrix, "Family of multiport bidirectional dc-dc converters," *Inst. Electr. Eng. Proc. Elect. Power Appl.*, vol. 153, no. 15, pp. 451–458, May 2006.

[5] Z. Qian, O. Abdel-Rahman, H. Al-Atrash, and I. Batarseh, "Modeling and control of three-port DC/DC converter interface for satellite applications," *IEEE Trans. Power Electron.*, vol. 25, no. 3, pp. 637–649, Mar. 2010.

[6] H. Tao, J. L. Duarte, and A. M. Marcel, "Three-port triple-half-bridge bidirectional converter with zero-voltage switching," *IEEE Trans. Power Electron.*, vol. 23, no. 2, pp. 782–792, Mar. 2008.

[7] H. Tao, A. Kotsopoulos, J. Duarte, and M. Hendrix, "Transformer-coupled multiport ZVS bidirectional dc-dc converter with wide input range," *IEEE Trans. Power Electron.*, vol. 23, no. 2, pp. 771–781, Mar. 2008.

[8] S. Falcones and R. Ayyanar, "Simple control design for a three-port DCDC converter based PV system with energy storage," presented at the IEEE Appl. Power Electron Conf , Palm Springs, CA, 2010

[9] H. Al-Atrash and I. Batarseh, "Boost-integrated phase-shift full-bridge converter for three-port interface," in

Proc. IEEE Power Electron. Spec. Conf., 2007, pp. 2313–2321.

[10] Z. Wang and H. Li, "Integrated MPPT and bidirectional battery charger for PV application using one multiphase interleaved three-port DC-DC converter," in *Proc. 26th IEEE Appl. Power Electron. Conf. Expo.*, 2011, pp. 295–300.

[11] S. Lim and A. Q. Huang, "Design of a transient voltage clamp (TVC) for 4 switch buck boost (4SBB) converter," in *Proc. IEEE Energy Convers. Congr. Expo*, 2009, pp. 659–661.

[12] E. Kim and Y. Kim, "A ZVZCS PWM FB DC/DC converter using a modified energy-recovery snubber," *IEEE Trans. Ind. Electron.*, vol. 49, no. 5, pp. 1120–1127, Oct. 2002.

[13] B.-Y. Chen and Y. S. Lai, "Switching control technique of phase-shift controlled full-bridge converter to improve efficiency under light-load and standby conditions without additional auxiliary components," *IEEE Trans. Power Electron.*, vol. 25, no. 4, pp. 1001–1012, Apr. 2010.

[14] A. Khaligh, J. Cao, and Y. Lee, "A multiple input DC-DC converter topology," *IEEE Trans. Power Electron.*, vol. 24, no. 3, pp. 862–868, Mar. 2009.

AUTHOR BIOGRAPHY

Dr. A.N. MALLESWARA RAO received B.E. in Electrical and Electronics Engineering from A.U, Waltair, India in 1999, M.Tech in Electrical Engineering from JNTUH, Hyderabad, India., and PhD from JNT University, Hyderabad, India in 2013. Presently, he is professor in Electrical & Electronics Engineering in SKEC, Khammam. Prof. Rao is an author of 12journal and conference papers. His research and study interests include power quality and power electronics.